

AD-754 203

VHF TO EHF PERFORMANCE OF A 90-FOOT
QUASI-TAPERED ANECHOIC CHAMBER

Robert B. Dybdal, et al

Aerospace Corporation

Prepared for:

Space and Missile Systems Organization

28 December 1972

DISTRIBUTED BY:

NTIS

National Technical Information Service
U. S. DEPARTMENT OF COMMERCE
5285 Port Royal Road, Springfield Va. 22151

VH

AIR FORCE REPORT NO.
SAMSO-TR-72-300

AEROSPACE REPORT NO.
TR-0073 (3230-40)-2

AD754203

VHF to EHF Performance of a 90-Foot Quasi-Tapered Anechoic Chamber

Prepared by R. B. DYBDAL and C. O. YOWELL
Electronics Research Laboratory

72 DEC 28

DDC
RECEIVED
JAN 23 1973
REGISTERED

Laboratory Operations
THE AEROSPACE CORPORATION

Prepared for SPACE AND MISSILE SYSTEMS ORGANIZATION
AIR FORCE SYSTEMS COMMAND
LOS ANGELES AIR FORCE STATION
Los Angeles, California

Reproduced by
NATIONAL TECHNICAL
INFORMATION SERVICE
U.S. Department of Commerce
Springfield, VA 22151

APPROVED FOR PUBLIC RELEASE: DISTRIBUTION UNLIMITED

89

125

ACC...	
KTIS	W H Division <input checked="" type="checkbox"/>
F D	Res Section <input type="checkbox"/>
Justification	<input type="checkbox"/>
BY	
USE RESTRICTION/AVAILABILITY CODES	
CLASS	AIR. & J. SPECIAL
A	

LABORATORY OPERATIONS

The Laboratory Operations of The Aerospace Corporation is conducting experimental and theoretical investigations necessary for the evaluation and application of scientific advances to new military concepts and systems. Versatility and flexibility have been developed to a high degree by the laboratory personnel in dealing with the many problems encountered in the nation's rapidly developing space and missile systems. Expertise in the latest scientific developments is vital to the accomplishment of tasks related to these problems. The laboratories that contribute to this research are:

Aerodynamics and Propulsion Research Laboratory: Launch and reentry aerodynamics, heat transfer, reentry physics, propulsion, high-temperature chemistry and chemical kinetics, structural mechanics, flight dynamics, atmospheric pollution, and high-power gas lasers.

Electronics Research Laboratory: Generation, transmission, detection, and processing of electromagnetic radiation in the terrestrial and space environments, with emphasis on the millimeter-wave, infrared, and visible portions of the spectrum; design and fabrication of antennas, complex optical systems and photolithographic solid-state devices; test and development of practical superconducting detectors and laser devices and technology, including high-power lasers, atmospheric pollution, and biomedical problems.

Materials Sciences Laboratory: Development of new materials; metal matrix composites and new forms of carbon; test and evaluation of graphite and ceramics in reentry; spacecraft materials and components in radiation and high-vacuum environments; application of fracture mechanics to stress corrosion and fatigue-induced fractures in structural metals; effect of nature of material surfaces on lubrication, photosensitization, and catalytic reactions, and development of prosthesis devices.

Plasma Research Laboratory: Reentry physics and nuclear weapons effects; the interaction of antennas with reentry plasma sheaths; experimentation with thermonuclear plasmas; the generation and propagation of plasma waves in the magnetosphere; chemical reactions of vibrationally excited species in rocket plumes; and high-precision laser ranging.

Space Physics Laboratory: Aeronomy; density and composition of the atmosphere at all altitudes; atmospheric reactions and atmospheric optics; pollution of the environment; the sun, earth's resources; meteorological measurements; radiation belts and cosmic rays; and the effects of nuclear explosions, magnetic storms, and solar radiation on the atmosphere.

THE AEROSPACE CORPORATION
El Segundo, California

DOCUMENT CONTROL DATA - R & D		
<i>(Security classification of title, body of abstract and indexing annotation must be entered when the overall report is classified)</i>		
1 ORIGINATING ACTIVITY (Corporate author) The Aerospace Corporation El Segundo, California		2a REPORT SECURITY CLASSIFICATION Unclassified
		2b GROUP
3 REPORT TITLE VHF TO EHF PERFORMANCE OF A 90-FOOT QUASI-TAPERED ANECHOIC CHAMBER		
4 DESCRIPTIVE NOTES (Type of report and inclusive dates)		
5 AUTHOR(S) (First name, middle initial, last name) Robert B. Dybdal and Cleyon O. Yowell		
6 REPORT DATE 72 DEC 28	7a TOTAL NO OF PAGES 25	7b NO OF REFS 9
8a CONTRACT OR GRANT NO F04701-72-C-0073	9a ORIGINATOR'S REPORT NUMBER(S) TR-0073(3230-40)-2	
b PROJECT NO.	9b OTHER REPORT NO(S) (Any other numbers that may be assigned this report) SAMSO-TR-72-300	
c		
d		
10. DISTRIBUTION STATEMENT Approved for public release; distribution unlimited.		
11 SUPPLEMENTARY NOTES	12. SPONSORING MILITARY ACTIVITY Space and Missile Systems Organization Air Force Systems Command Los Angeles, California	
13 ABSTRACT <p>The measured reflection characteristics of a 90-ft anechoic chamber operated by The Aerospace Corporation are reported. The design of this chamber, described as quasi-tapered, is unique in that it tapers from a large rectangular test region to a smaller square transmitting end. This design incorporates the performance advantages of a fully tapered chamber at low frequencies with some of the flexibility of a rectangular chamber when used at higher frequencies. The performance of this chamber is reported from 100 MHz to 93 GHz.</p> <p>Details of illustrations in this document may be better studied on microfiche.</p>		

UNCLASSIFIED

Security Classification

14

KEY WORDS

Radar cross section measurements
VHF radiation measurements
EHF radiation measurements
Microwave anechoic chamber

Distribution Statement (Continued)

Abstract (Continued)

I-8

UNCLASSIFIED
Security Classification

Air Force Report No.
SAMSO-TR-72-300

Aerospace Report No.
TR-0073(3230-40)-2

VHF TO EHF PERFORMANCE OF A 90-FOOT
QUASI-TAPERED ANECHOIC CHAMBER

Prepared by
R. B. Dybdal and C. O. Yowell
Electronics Research Laboratory

72 DEC 28

Laboratory Operations
THE AEROSPACE CORPORATION

Prepared for
SPACE AND MISSILE SYSTEMS ORGANIZATION
AIR FORCE SYSTEMS COMMAND
LOS ANGELES AIR FORCE STATION
Los Angeles, California

Approved for public release;
distribution unlimited

I-C

FOREWORD

This report is published by The Aerospace Corporation, El Segundo, California, under Air Force Contract No. F04701-72-C-0073.

This report, which documents research carried out from July 1970 to July 1972, was submitted on 27 November 1972 to Lt Col Elliott W. Porter, DYX, for review and approval.

It is the authors' pleasure to acknowledge the assistance of their colleagues in the Electronics Research Laboratory, particularly H. E. King, J. L. Wong, and R. D. Etcheverry and to thank L. U. Brown for performing the measurements.

Approved



A. H. Silver, Director
Electronics Research Laboratory

Publication of this report does not constitute Air Force approval of the report's findings or conclusions. It is published only for the exchange and stimulation of ideas.



ELLIOTT W. PORTER, Lt Colonel, USAF
Executive Officer
Deputy for Technology

CONTENTS

I. INTRODUCTION	1
II. VHF MEASUREMENTS	5
III. MILLIMETER-WAVE MEASUREMENTS	11
IV. SUMMARY	15
REFERENCES	17
APPENDIX	19

Preceding page blank

FIGURES

1.	Geometry of Anechoic Chamber	2
2.	Anechoic Chamber Characteristics	3
3.	VHF Radar in Anechoic Chamber	6
4.	Block Diagram of VHF Radar Equipment	7
5.	Broadside RCS of Short-Circuited Dipole	8
6.	Canceled Background RCS at VHF	9
7.	Sphere-Cone Target in Anechoic Chamber	12
8.	Measured RCS of Sphere-Cone at 93 GHz	13
9.	Calculated RCS of Sphere-Cone at 93 GHz	14
A-1.	Geometry of the Sphere-Cone	20

TABLES

1.	Chamber Evaluation with the Use of Calibration Spheres . . .	8
A-1.	Scattered "Field" Values	21
A-2.	Phase Reference for Scattering Centers	21

I. INTRODUCTION

Although anechoic chamber design has received much attention, documentation of the performance of an anechoic chamber using VHF absorber on the back wall is not presently available over a wide range of frequencies. The purpose of this report is to describe the measured characteristics of a 90-ft long anechoic chamber for frequencies from 100 MHz to 93 GHz.

The chamber configuration is illustrated in Fig. 1 and is described as a quasi-tapered design (Ref. 1). The $19 \times 21 \times 30$ -ft test region is linearly tapered into a smaller 8×8 -ft transmitting end. A tapered chamber has been shown to produce a more uniform field distribution in the quiet zone than a rectangular chamber (Ref. 2); however, excitation of a fully tapered chamber is relatively complex (Ref. 3) and a quasi-monostatic configuration for radar cross section (RCS) measurements is difficult to implement. The quasi-tapered design combines the performance advantages of a fully tapered chamber when used at low frequencies with some of the instrumentation flexibility of a rectangular chamber. Prior to constructing the anechoic chamber, measurements were performed on a model chamber (Ref. 4) to verify an acceptable performance.

The anechoic chamber was constructed by B. F. Goodrich and their RF evaluation is contained in Ref. 5. The rear wall of the chamber is covered with 70-in. thick pyramidal absorber (VHP-70). This wall is tiltable up to 6 deg from vertical to reduce the chamber background level, a technique that is particularly useful at the higher frequencies. The walls of the test region (quiet zone) are lined with 18-in. pyramidal absorber (VHP-18), and the tapered section is lined with 14-in. wedge absorber (WG-14).

The measured background RCS level for an equivalent target at a 50-ft range and the reflectivity of the chamber for frequencies between 100 MHz and 93 GHz are summarized in Fig. 2. Since anechoic chamber performance at microwave frequencies has been reported elsewhere, emphasis in the remainder of this discussion is placed on VHF and millimeter-wave measurements.

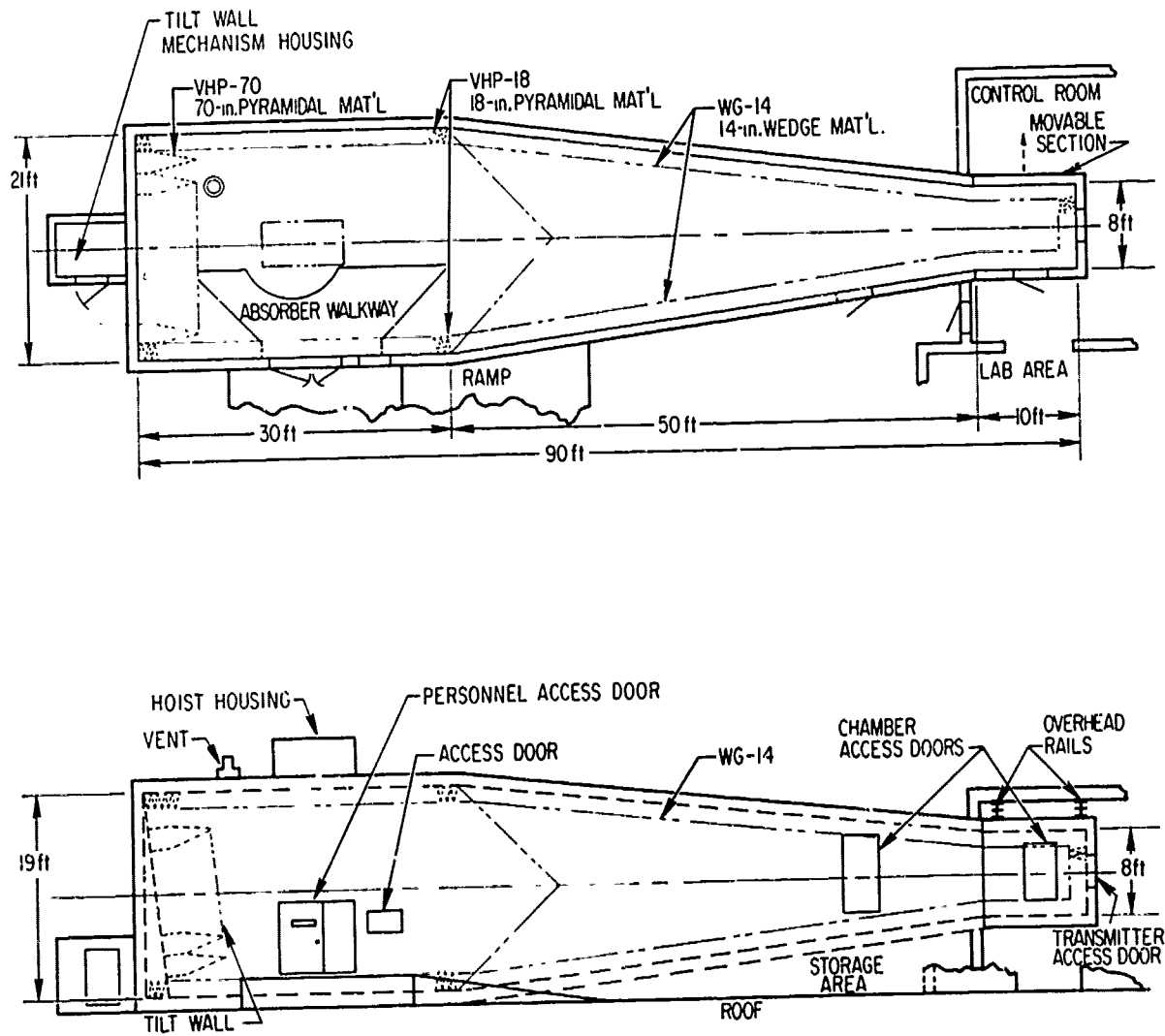


Fig. 1. Geometry of Anechoic Chamber

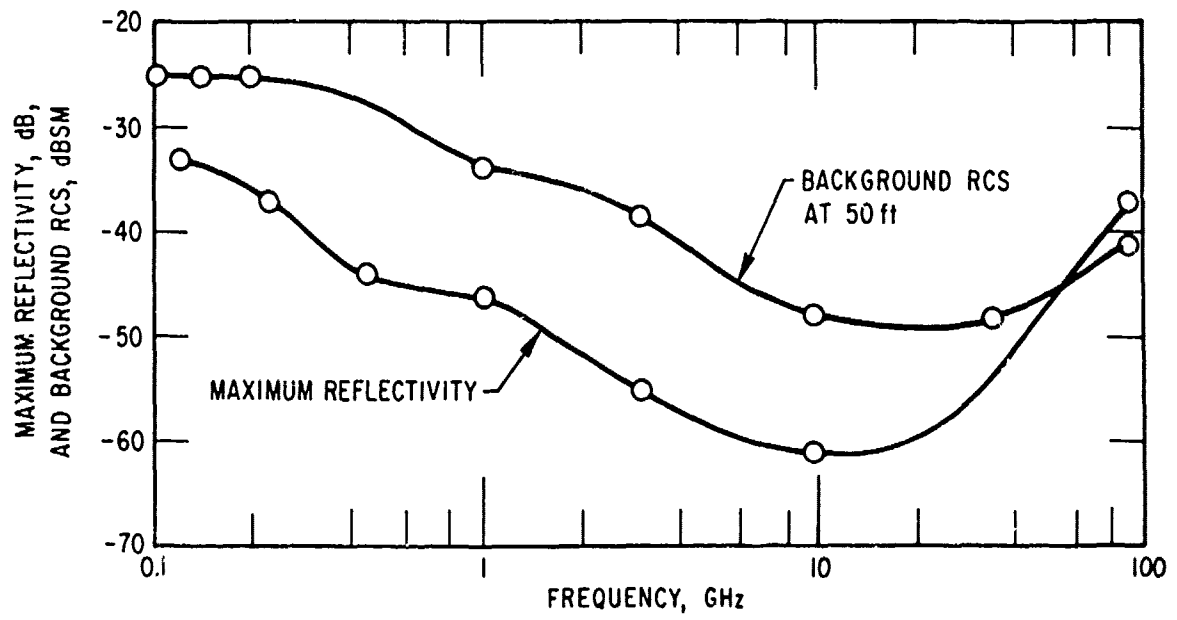


Fig. 2. Anechoic Chamber Characteristics

II. VHF MEASUREMENTS

Recently, measurements have been performed on electrically small, impedance-loaded targets at VHF.¹ As a part of this program, the anechoic chamber was evaluated for frequencies between 100 and 200 MHz. In these measurements, a log periodic antenna located 25 ft from the target, as shown in Fig. 3, was used for transmitting and receiving. The rest of the equipment used in the radar is illustrated in Fig. 4. This range was selected to minimize the isolation required of the Anzac H-1 hybrid. An HP 5105A synthesizer provided a convenient, stable source for these measurements. Chamber background cancellation was achieved by using both the fourth port of the hybrid and a cancellation path between the receiver and transmitter. Most of the "background" stems from the hybrid unbalance rather than from anechoic chamber reflections. Hybrid unbalance was caused by antenna mismatch, and no attempt was made to match the antenna over a wide frequency range.

The chamber was evaluated in three ways: (1) the field in the quiet zone was probed using a corner reflector antenna, (2) the differential RCS of two calibration spheres was measured, and (3) the measured broadside response of a short-circuited dipole was compared with a theoretical result. At the target range, the amplitude variation of the field along the chamber axis was 0.7 dB and the phase slope was linear, having a value of 177 deg/meter as compared with 180 deg/meter for a 150 MHz plane wave. The field measured within ± 2 ft of the axis varied in amplitude by 0.5 dB and 8 deg in phase. The measurements indicate a good plane wave is excited over a small test region even when the transmit/receive antenna is placed halfway down the taper of the chamber. The differential RCS between 12- and 20-in. diameter calibration spheres was measured between 110 and 180 MHz, and the average difference between theoretical and measured results is given in Table 1. Finally, the broadside response of a short-circuited dipole was measured, as shown in Fig. 5, and the results compared with the theoretical values published by Harrington (Ref. 6).

¹R. B. Dybdal and C. O. Yowell, Radar Cross Section Characteristics of Impedance-Loaded Targets, Aerospace Corporation Technical Report (1973).

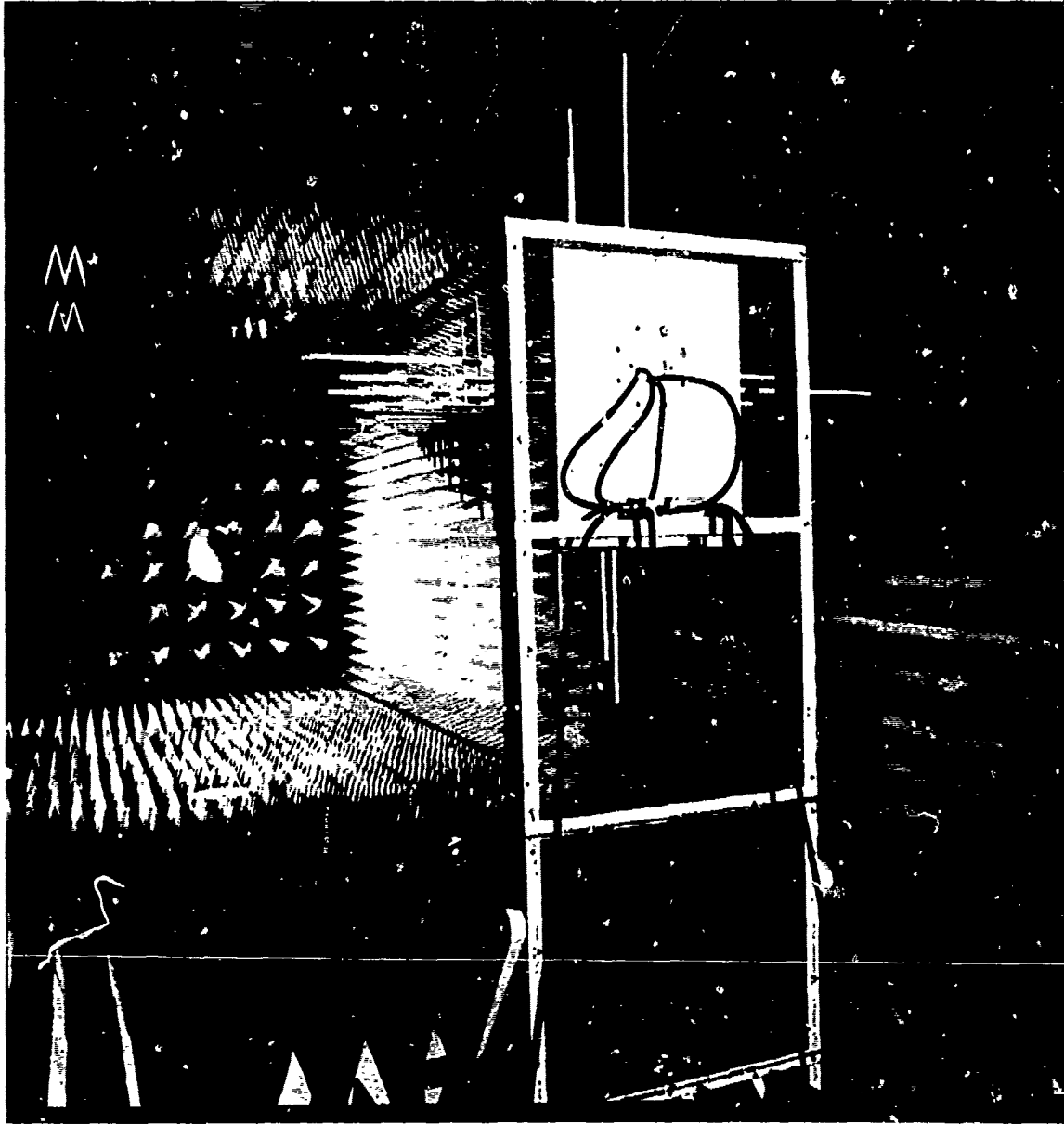


Fig. 3. VHF Radar in Anechoic Chamber

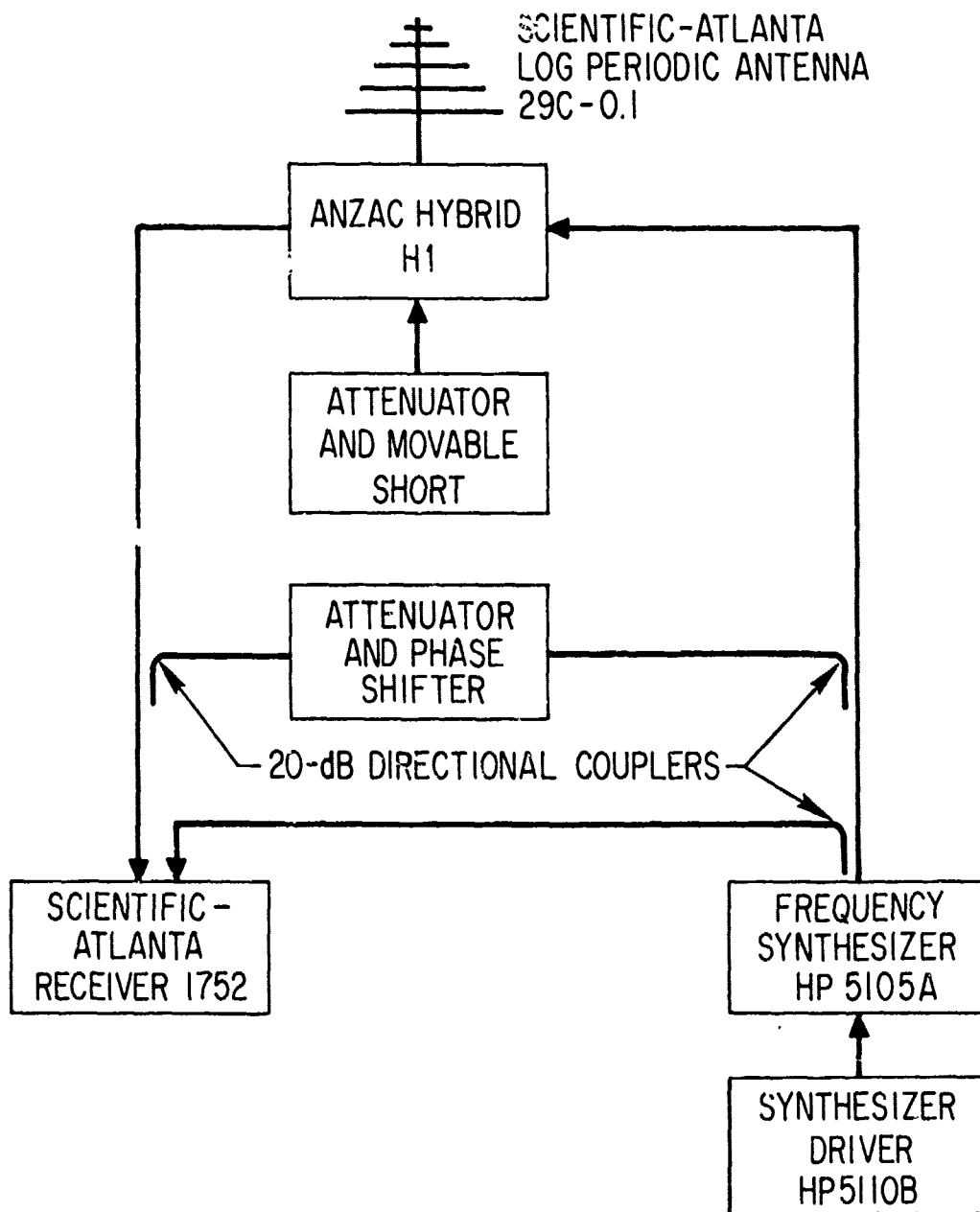


Fig. 4. Block Diagram of VHF Radar Equipment

Reproduced from
best available copy.

Table 1. Chamber Evaluation with the Use of Calibration Spheres

Frequency (MHz)	σ 20-In. Sphere (dBsm)	$\frac{\sigma_{20\text{-In. Sphere}}}{\sigma_{12\text{-In. Sphere}}}$			Average Deviation (dB)
		Calculated (dB)	Measured, 10/19/71 (dB)	Measured, 10/21/71 (dB)	
110	-7	12.8		11.8	-1.0
120	-5.9	12.6	12.2	12.0	-0.5
130	-4.6	12.4	11.8	12.0	-0.5
140	-3.7	12.3	11.9	10.5	-1.1
145	-3.2	12.1	11.8		-0.3
150	-2.8	12.0	12.0	10.2	-0.9
155	-2.5	11.8	12.0		+0.2
160	-2.2	11.6	12.0	11.3	+0.05
170	-1.8	11.0	10.2	11.2	-0.3
180	-1.4	10.4	11.2	11.0	+0.7

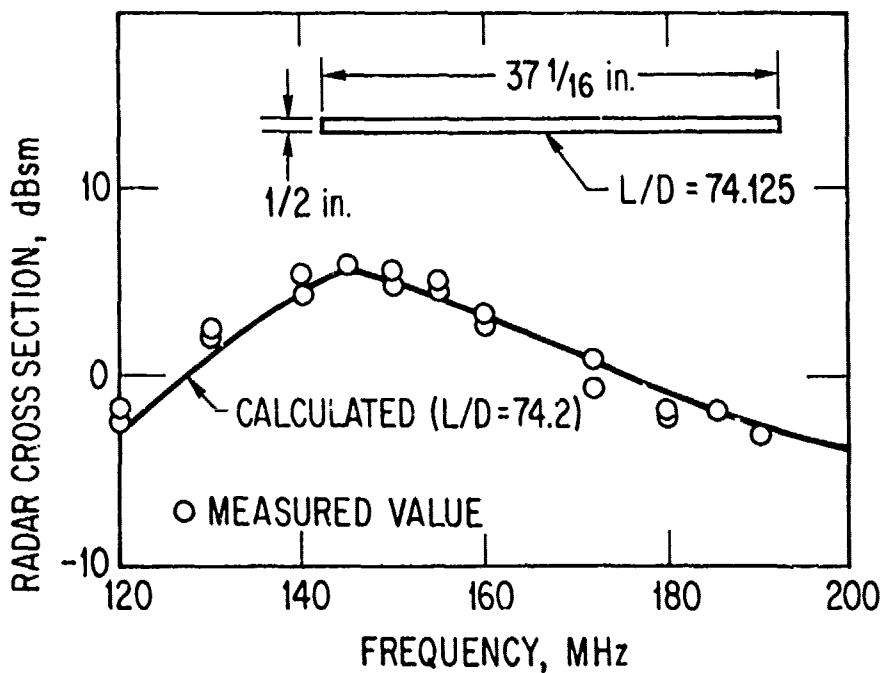


Fig. 5. Broadside RCS of Short-Circuited Dipole

During the course of the measurements on impedance-loaded targets, the canceled background levels of the anechoic chamber were recorded after the target measurements were performed. A plot of 81 representative measurements is given in Fig. 6. The relatively large spread in these values is the result of the varying time durations and amounts of disturbance in the chamber during the measurements. The initial canceled values prior to target measurement over this frequency range were in excess of -45 dBsm referenced to a range of 25 ft. No special efforts were made to stabilize either mechanically or thermally the long coaxial lines used in the bridge balancing circuit.

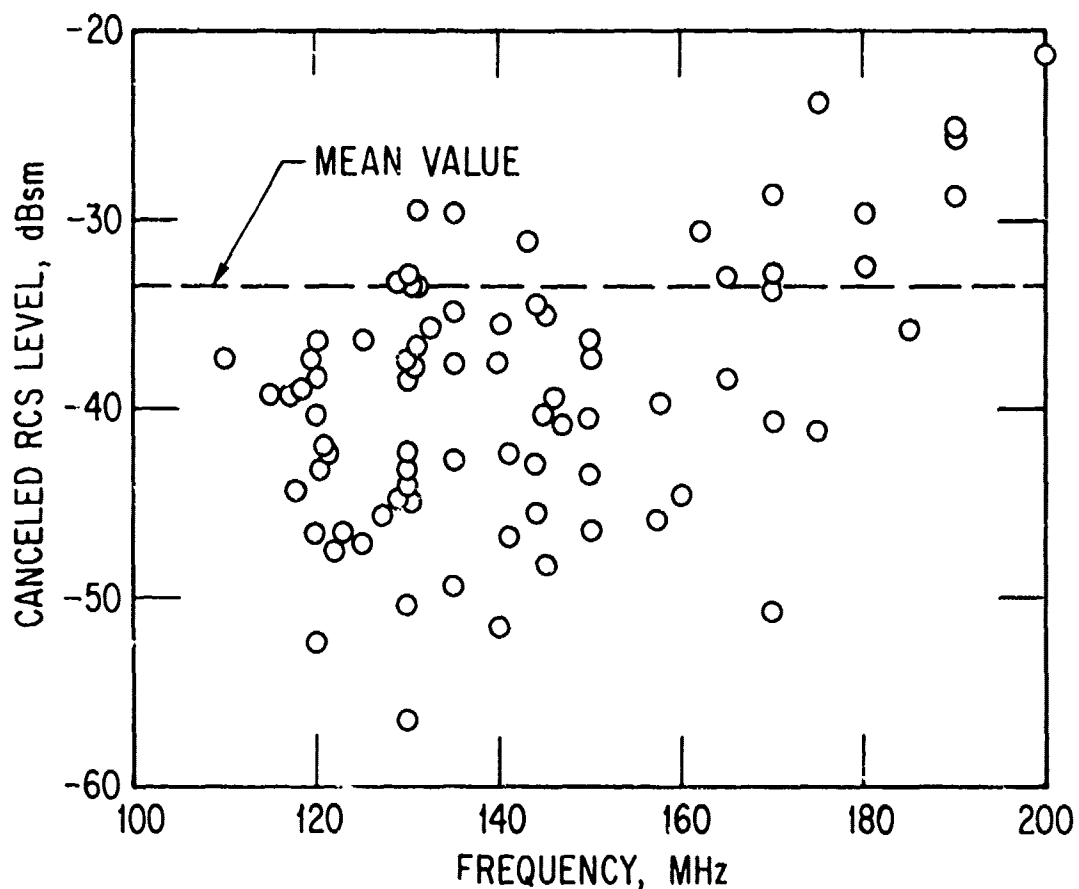


Fig. 6. Canceled Background RCS at VHF

III. MILLIMETER-WAVE MEASUREMENTS

The millimeter-wavelength frequency range affords the possibility of performing scaled frequency measurements on physically small models. Such models are readily constructed and easily maneuvered. The Aerospace chamber has been operated at 93 GHz which, to the best knowledge of the author, is the highest frequency used in a microwave chamber. The phase-locked transmitter and receiver used in these measurements have been converted from equipment used to measure the phase structure function of the atmosphere (Ref. 7).

Prior to constructing the chamber, measurements were performed at 94 GHz on readily available absorber material (Ref. 8). Results of these measurements indicate that the sharpness of absorber tips is important and some protective absorber paints reflect significantly. Consequently, the absorber tips on the rear wall were left unpainted and specified as "extra sharp." The background RCS and reflectivity properties of the anechoic chamber at 93 GHz have been previously reported (Ref. 9).

To illustrate a scale-model measurement performed at EHF, a sphere-cone target (shown in Fig. 7) was measured in the anechoic chamber. This target is 4 in. long with a 1/2-in. nose radius and a 2-in. base diameter. The target was supported by monofilament lines as shown, and horizontal polarization is used in the measurements since even 2-lb test monofilament has a peak specular return for vertical polarization of -20 dBsm at these frequencies. However, model dimensions in this frequency range are generally large in terms of wavelengths, and polarization dependence is not significant in specular regions.

The RCS of the sphere-cone target, measured at 93 GHz, is given in Fig. 8. The calculated RCS for this target, based on an approximate physical optics analysis described in the Appendix, is given in Fig. 9. The agreement between measured and calculated results is quite good in the specular regions.

At low RCS levels, the measured pattern accuracy is limited by the chamber background level, and the calculated levels (as predicted by the physical optics analysis) are probably not altogether valid since some polarization dependence should be observed.

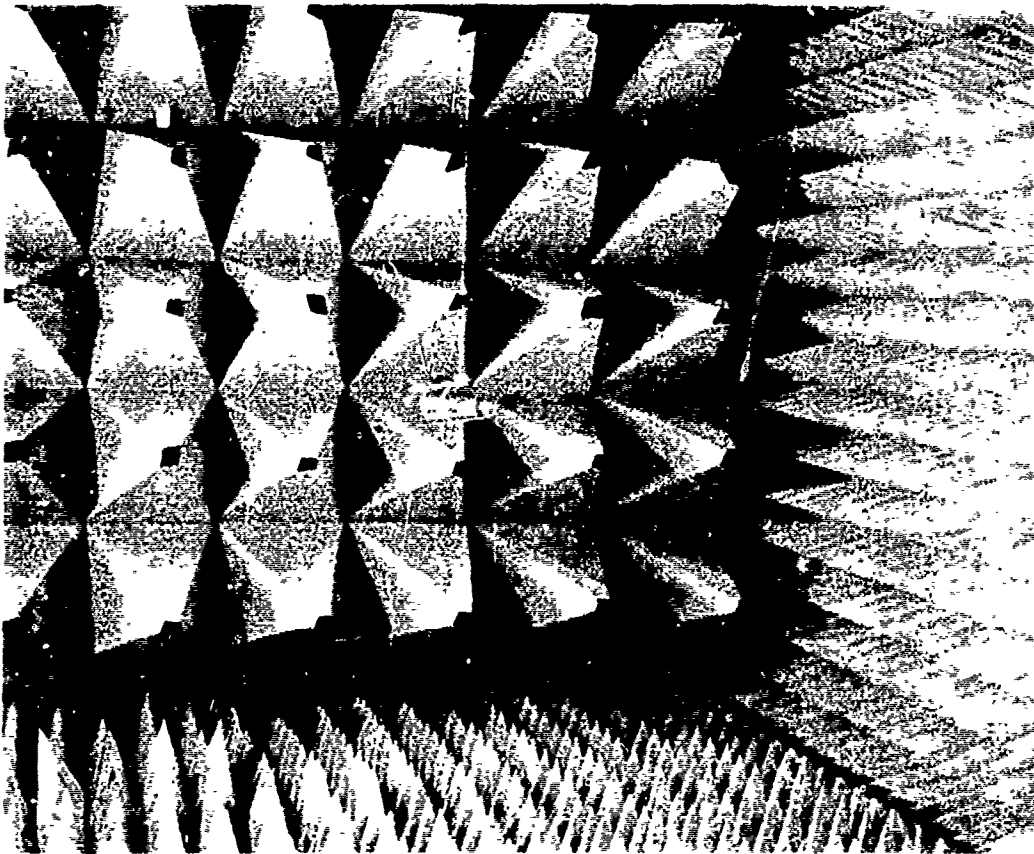


Fig. 7. Sphere-Cone Target in Anechoic Chamber

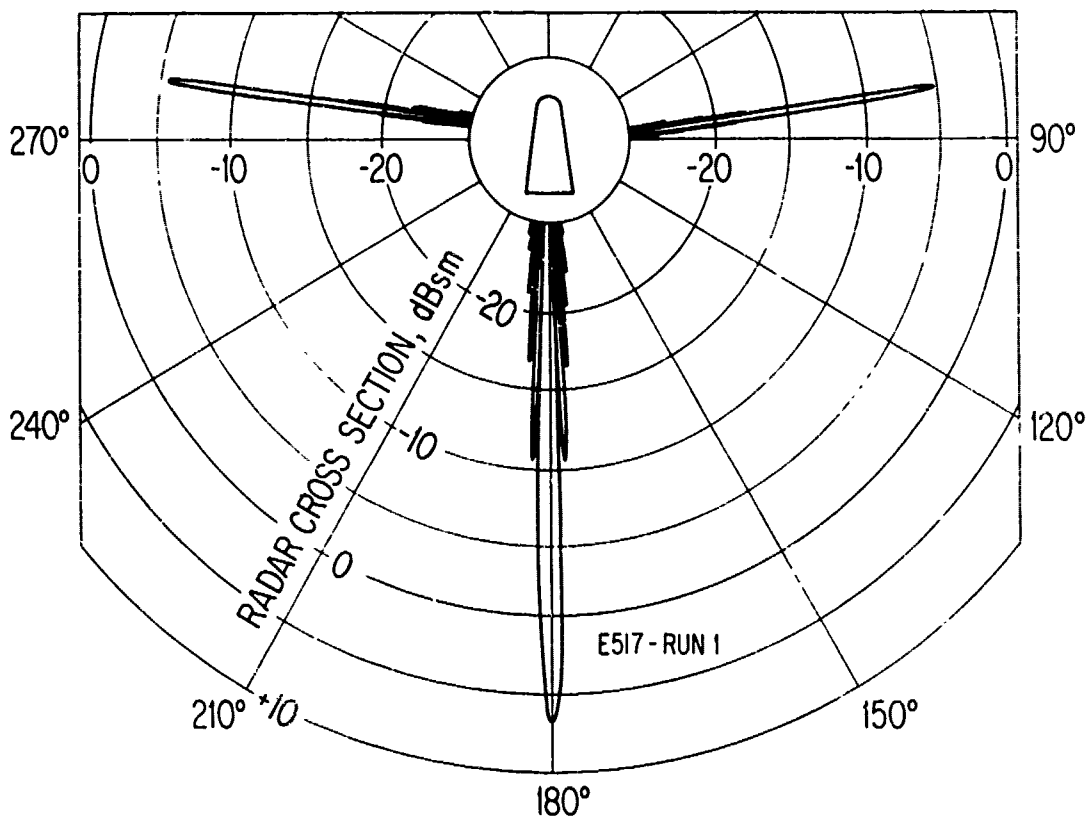


Fig. 8. Measured RCS of Sphere-Cone at 93 GHz

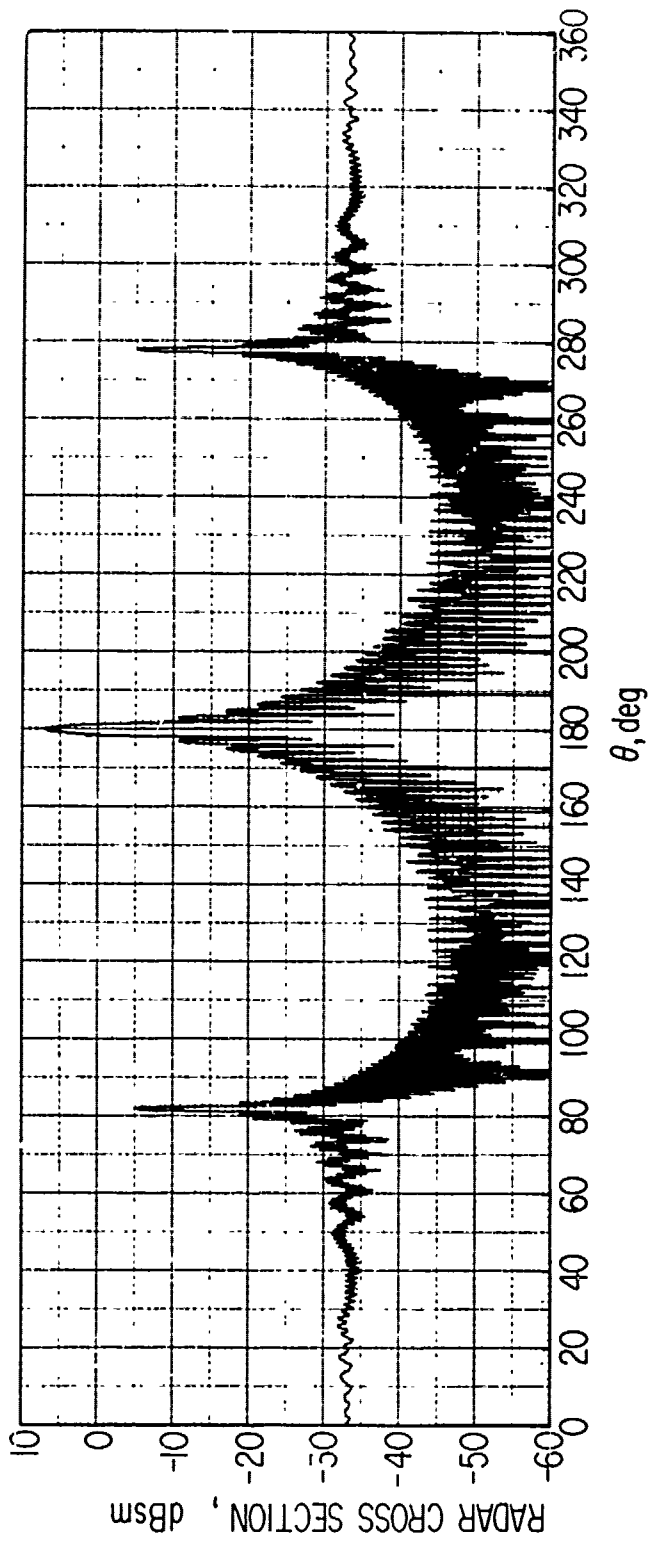


Fig. 9. Calculated RCS of Sphere-Cone at 93 GHz

IV. SUMMARY

Some measured characteristics of a 90-ft anechoic chamber have been presented illustrating its usefulness over a broad range of frequencies from VHF to EHF. The quasi-tapered design permits flexibility in equipment arrangements while retaining the performance advantages of a fully tapered design. VHF RCS measurements between 100 and 200 MHz are described. The RCS of a scaled sphere-cone target recorded at 93 GHz demonstrates the feasibility of millimeter-wavelength measurements in an anechoic chamber.

REFERENCES

1. R. B. Dybdal, H. E. King, J. L. Wong, and C. O. Yowell, Performance of a 90-Foot Quasi-Tapered Anechoic Chamber: 120 MHz to 93 GHz, TR-0059(6230-30)-4, The Aerospace Corporation, El Segundo, Calif. (3 September 1970).
2. W. H. Emerson and H. B. Sefton, "An Improved Design for Indoor Ranges," Proc. IEEE 53 (8), 1079-1081 (August 1965).
3. R. L. Swan and J. Saldi, "A New Tapered Anechoic Chamber Illuminating Antenna," Nineteenth Annual Symposium USAF Antenna Research and Development Program, Robert Allerton Park, Illinois, Air Force Avionics Laboratory, 14-16 October 1969.
4. H. E. King, F. I. Shimabukuro, and J. L. Wong, "Characteristics of a Tapered Anechoic Chamber," IEEE Trans. on Antennas and Propagation AP-15 (3), 488-490 (May 1967). Also, Report No. TR-1001(2230-46)-2, The Aerospace Corporation, El Segundo, Calif. (February 1967).
5. Measurement of the 90-Ft Tapered Chamber at Aerospace Corporation, Report MR-42, B. F. Goodrich Sponge Products, Shelton, Connecticut (March 1969).
6. R. F. Harrington, Field Computation by Moment Methods, Macmillan Company, New York, New York (1968), p. 77.
7. R. D. Etcheverry, G. R. Heidbreder, W. A. Johnson, and H. J. Wintroub, "Measurements of Spatial Coherence in 3.2-mm Horizontal Transmission," IEEE Trans. on Antennas and Propagation AP-15 (1), 136-141 (January 1967).
8. H. E. King, F. I. Shimabukuro, and J. L. Wong, 94 Gc Measurement of Microwave Absorbing Material, TR-669(6230-46)-5, The Aerospace Corporation, El Segundo, Calif. (March 1966).
9. C. O. Yowell, "Reflection Characteristics of a 90-Ft Tapered Anechoic Chamber at 93 GHz," 1968 International Antenna and Propagation Symposium Digest, 259-267 (September 1968).

APPENDIX

A description is given in this Appendix of the approximate physical optics analysis used to calculate the EHF RCS of the sphere-cone target. The geometry of the sphere-cone target used in this analysis is presented in Fig. A-1. The model was specified using the overall length A (4 in.), the base radius a (1 in.), and the nose radius r (1/2 in.). The length of the conical portion L is given by

$$L = [A^2 + a^2 - 2Ar]^{1/2} \quad (A-1)$$

and the angle θ_1 by

$$\theta_1 = \sin^{-1} \left[\frac{La + r^2 - rA}{L^2 + r^2} \right] \quad (A-2)$$

This analysis assumes that the nose sphere and the conical frustum are attached with a tangent join.

The RCS σ may be computed by combining the cross-section components of the individual scattering centers in a phasor sum, and is expressed by

$$\sigma = \left| \sum_i U_i e^{-j\phi_i} \right|^2 \quad (A-3)$$

In this expression, U_i represents the scattered "field" components of the individual scattering centers and ϕ_i is the phase of the individual scattering centers referenced to a common point. The physical optics approximation will be used to obtain the scattered field components. Since RCS is

a scattered power expression, the square root of the RCS of the individual scattering centers will be used to obtain scattered "field" components.

For the sphere-cone target, three scattering centers will be used: (1) the flat disk response for the base, (2) a sphere response for the nose, and (3) an approximate response for the conical frustum. Physical optics is used to obtain the responses for these scattering centers. The approximate response for the conical frustum assumes a $\sin X/X$ functional form coinciding with the specular direction of the frustum and the amplitude assumes that of a cylinder having the average radius of the frustum. The scattered "field" values for the three scattering centers are given in Table A-1. The phase of the scatterers, referenced to the center of the base, is given in Table A-2. This analysis was programmed and the results are shown in Fig. 9.

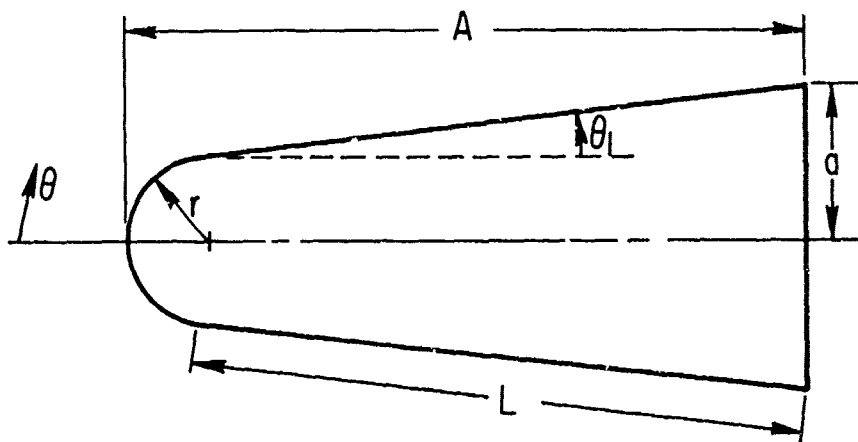


Fig. A-1. Geometry of the Sphere-Cone

Table A-1. Scattered "Field" Values

Scatterer	Illumination Region (deg)	Value
Sphere (nose)	$-90 + \theta_1 < \theta < 90 - \theta_1$	$U_1 = r\sqrt{\pi}$
Frustum	$-180 + \theta_1 < \theta < 180 - \theta_1$	$U_2 = L \sqrt{\frac{\pi(a + r \cos \theta_1)}{\lambda}} \sin(\theta + \theta_1)$ $\times \frac{\sin X_1}{X_1}$ $X_1 = \frac{2\pi L}{\lambda} \cos(\theta + \theta_1)$
Disk (base)	$90 < \theta < 270$	$U_3 = \frac{4\pi^{3/2} a^2}{\lambda} \cos \theta \frac{J_1(X_2)}{X_2}$ <p>$J_1(X)$ - Bessel Function of Order 1</p> $X_2 = \frac{4\pi a}{\lambda} \sin \theta$

Table A-2. Phase Reference for Scattering Centers

$$\phi_1 = \frac{4\pi}{\lambda} [r + (A - r) \cos \theta]$$

$$\phi_2 = \frac{2\pi}{\lambda} [(a + r \cos \theta_1) \sin \theta + (A - r(1 - \sin \theta_1)) \cos \theta]$$

$$\phi_3 = 0$$